Effects of block copolymer's architecture on its association with lipid membranes: Experiments and simulations

Shelli L. Frey
Department of Chemistry, Institute for Biophysical Dynamics and James Franck Institute, The University of Chicago, Chicago, Illinois 60637, USA

Dongsheng Zhang, Marcelo A. Carignano, and Igal Szleifer[a)]
Department of Chemistry, Purdue University, 560 Oval Drive, West Lafayette, Indiana 47907-1393, USA

Ka Yee C. Lee[b)]
Department of Chemistry, Institute for Biophysical Dynamics and James Franck Institute, The University of Chicago, Chicago, Illinois 60637, USA

(Received 20 March 2007; accepted 12 July 2007; published online 20 September 2007)

Triblock copolymers of the form poly(ethylene oxide)-poly(propylene oxide)-poly(ethylene oxide) (PEO-PPO-PEO) have been shown to effectively interact with and restore activity of damaged cell membranes. To better understand the interaction between these polymers and cell membranes, we have modeled the outer leaflet of a cell membrane with a lipid monolayer spread at the air-water interface and injected poloxamers of varying architectures into the subphase beneath the monolayer. Subsequent interactions of the polymer with the monolayer upon compression were monitored with concurrent Langmuir isotherm and fluorescence microscopy measurements. Monte Carlo simulations were run in parallel using a coarse-grained model to capture interactions between lipids and poloxamers. Changing the ratio of the PEO to PPO block lengths (N_{PEO}:N_{PPO}) affects the equilibrium spreading pressure of the polymer. Poloxamers with a relatively longer central hydrophobic block are less soluble, resulting in more polymer adsorbed to the interface and therefore a higher equilibrium spreading pressure. Simulation results show that changing the poloxamer structure effectively affects its solubility. This is also reflected in the degree of lipid corralling as poloxamers with a higher chemical potential (and resulting higher equilibrium spreading pressure) cause the neighboring lipid domains to be more ordered. Upon lateral compression of the monolayers, the polymer is expelled from the film beyond a certain squeeze-out pressure. A poloxamer with a higher N_{PEO}:N_{PPO} ratio (with either N_{PEO} or N_{PPO} held constant in each series) has a lower squeeze-out pressure. Likewise when the total size of the polymer is varied with a constant hydrophilic:hydrophobic ratio, smaller poloxamers are squeezed out at a lower pressure. Our simulation results capture the trends of our experimental observations, both indicating how the interactions between lipids and poloxamers can be tuned by the polymer architecture. [DOI: 10.1063/1.2768947]

I. INTRODUCTION

[12]Triblock copolymers of the form poly(ethylene oxide)-poly(propylene oxide)-poly(ethylene oxide) (PEO-PPO-PEO) are a class of surface active amphiphilic molecules.[1] These commercially available noncytotoxic, nonionic agents are commonly referred to as poloxamers. Poloxamers have an extensive range of applications in the medical field such as drug solubilization, controlled release, and protection of microorganisms against mechanical damage.[2–4] Of particular interest is F68 (also known as P188), a specific poloxamer of the form PEO_{76}-PPO_{29}-PEO_{76}, which has been proven as a sealing agent for permeabilized lipid membranes. Increased cell permeability accounts for the majority of tissue damage in common clinical conditions after physicochemical insults such as electrical shock, significant radiation damage, thermal burns, and frostbite. The efficacy of F68 was first shown to reduce the leakage of carboxyfluorescein dye from loaded cells after electroporation.[5] Further studies have shown that F68 also effectively seals the damaged membranes of fibroblasts after heat shock,[6] skeletal muscle cells exposed to high-dose radiation,[7] and neuronal cells after mechanical disruption,[8] arresting the leakage of intracellular components.

More recent studies indicate the effectiveness of various types of poloxamers as a pharmaceutical not only to seal membranes, but also restore flexibility to stiffened muscle cells, or selectively target cancer cells for gene therapy.[9,10] Even with the extensive number of medical applications using poloxamers, little is known about the mechanism and driving forces that mediate the polymer's interaction with, and subsequent expulsion from cells. To take a more controlled approach in the development of poloxamers as healing agents, one must understand the fundamental interactions

[a)]Permanent address: Department of Biomedical Engineering, Northwestern University, 2145 Sheridan Road, Evanston, IL 60208.
[b)]Author to whom correspondence should be addressed. Electronic mail: kayeelee@uchicago.edu

between poloxamer molecules and the cell membrane. Although cell membranes are composed of lipid bilayers, a Langmuir lipid monolayer serves as a good model for the outer leaflet of the membrane. This simplified system provides valuable insight towards the interaction between lipid membranes and various biologically relevant molecules ranging from peptides to polymers.[11–14] Results from surface pressure versus area per molecule isotherms indicate that F68 inserts into a single component dipalmitoylphosphatidylcholine (DPPC) or dipalmitoylphosphatidylglycerol lipid monolayer at its equilibrium spreading pressure, and upon compression, is squeezed out at a significantly higher pressure.[13] X-ray scattering techniques have provided molecular level evidence that poloxamers selectively insert into regions of low lipid density and corral nearby lipids to restore barrier function of the membrane. Upon compression of the monolayer, the poloxamer has been shown to be squeezed out when the integrity of the monolayer is reestablished.[15,16] Using Monte Carlo simulations, the conditions for diblock copolymer induced formation of corralled lipid domains with crystal-like order in two dimensions have been shown to be a size mismatch between the lipid tail and hydrophobic polymer component as well as a long-range soft repulsive interaction between the hydrophilic blocks of the polymer.[17] The effect of poloxamer structure has been explored using isotherm experiments which show polymers with larger hydrophobic central blocks have stronger penetration abilities into monolayers.[18]

The work reported here uses both experiments and simulations to address how poloxamer structure affects its interactions with lipid monolayers. Using a model lipid system, we have carried out isotherm measurements and fluorescence microscopy (FM) imaging to examine the interactions of various poloxamers with zwitterionic DPPC monolayers at an air-water interface. Pretreatment experiments have been performed where the poloxamer is incorporated into a low-density lipid monolayer and then the monolayer is compressed causing subsequent polymer squeeze-out, therefore modeling the interaction of poloxamers with the cell membrane and their eventual expulsion from the membrane. To further investigate the driving forces responsible for the observed membrane insertion and sealing capabilities of poloxamers, we have systematically varied the chain length of specific blocks to alter the overall structure and quantified the effect of this on polymer/lipid interactions. A detailed understanding of how the molecular architecture of a triblock copolymer affects its interactions with lipid films is essential in the development of poloxamer based biomedical techniques which can range from gene therapy to sealing injured cells.

The theoretical description of the lipid/polymer mixtures is a complex enterprise due to the large number of degrees of freedom in both types of molecules. An atomistic simulation of the ability of the polymers to corral the lipids is out of reach of current computational methodologies. Furthermore, we are interested in mimicking the compression of the layer as well as the adsorption of the poloxamers. Both processes occur on a time scale that goes beyond the capabilities of current atomistic computational methodologies. In order to elucidate the main physical origin of the role of the poloxamer in corralling the lipids, we have developed a coarse-grained model that captures the main physical interactions between the complex molecules. We have recently shown using the coarse-grained model that the conditions for the corralling of the lipids by the poloxamers are the size mismatch of the hydrophobic block of the polymer and the lipid tails and the soft long-range repulsions due to the hydrophilic PEO blocks.[17] In the work presented here we show how this same model provides a physical picture of the role of the block chain lengths in the observed pressure-area isotherms and the adsorption and expulsion of the polymer chains as the layer is compressed. The aim of the simulations is not a quantitative comparison with the experimental observations. Rather, the simulations are expected to provide the basic physical behavior that is responsible for the experimental observations. In this way, favorable comparisons of the trends measured in the experimental observations and the predictions of the simulations are expected to illustrate the physical interactions determining the behavior of the lipid-poloxamer mixtures.

The focus of this work is to determine the interaction of poloxamers with a lipid monolayer depending on the ratio of chain lengths, $N_{PEO}:N_{PPO}$ (hydrophilic:hydrophobic), as well as varying the total size of a poloxamer while maintaining a constant $N_{PEO}:N_{PPO}$ ratio. These variables affect the solubility of the poloxamer and therefore the partitioning of the polymer between the interface and the subphase. We show both experimentally and through Monte Carlo simulations that the $N_{PEO}:N_{PPO}$ ratio dictates the equilibrium spreading pressure (ESP) of the poloxamer at the interface. Poloxamers with a higher proportion of hydrophobic blocks are less soluble, resulting in more poloxamers adsorbed to the interface, and therefore a higher ESP. Simulations show that changing the poloxamer structure leads to differences in subphase solubility that is also reflected in the degree of lipid corralling where poloxamers with a higher chemical potential (and resulting higher ESP) cause the lipid domains to be more ordered. Upon compression of the monolayer leading to expulsion of the polymer from the film, a poloxamer with a higher $N_{PEO}:N_{PPO}$ ratio favors a lower squeeze-out pressure. Likewise, when the total size of the polymer is varied but the hydrophilic:hydrophobic ratio is constant, a smaller poloxamer is squeezed out at a lower pressure.

II. MATERIALS AND METHODS

A. Lipids and subphase

DPPC was obtained in powder form from Avanti Polar Lipids, Inc. (Alabaster, AL) and used without further purification. The fluorescent probe used for visualization with FM was Texas Red labeled 1,2-dihexadecanoyl-sn-glycerol-3-phosphoethanolamine (TR-DHPE) (Molecular Probes, Eugene, OR). Monolayer spreading solutions were prepared by dissolving DPPC in chloroform (high-performance liquid chromatography grade, Fisher Scientific, Pittsburgh, PA) at a concentration of 0.2 mg/ml and adding 0.5 mol % of TR-DHPE. Lipid solutions were stored at −20 °C in glass vials. For all Langmuir trough experiments, the subphase was ul-

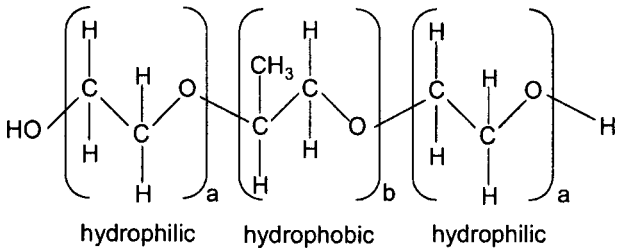

FIG. 1. Chemical structure of poloxamers consisting of poly(ethylene oxide) (PEO) and poly(propylene oxide) (PPO) blocks. The series of different poloxamers is constituted through varying numbers and ratios for (a) (N_{PEO}) and (b) (N_{PPO}).

trapure water (resistivity $\geqslant 18\ M\Omega\ cm$) processed by a Milli-Q ultrapurification system (A-10 gradient, Millipore, Bedford, MA).

B. Poloxamer solutions

Solutions of each poloxamer (F65, F84, F85, F88, F105, and F123) (BASF, Parsippany, NJ) (Fig. 1 and Table I) were made by mixing 200 mg of the poloxamer per milliliter of water in a vial with a magnetic stir bar for up to 60 min to ensure complete dissolution. All poloxamer solutions were stored at 4 °C and made fresh weekly. In the naming system of the poloxamers established by BASF, the final digit indicates the percent by weight of the hydrophilic block and the leading numbers multiplied by 300 provides the hydrophobe molecular weight. For example, F88 is 80% PEO by weight and the PPO block molecular weight is 2400 g/mol meaning PEO_{109}-PPO_{41}-PEO_{109} and a total molecular weight of 12 000 g/mol.

C. Equipment

Surface pressure-area isotherms were obtained using a custom-made Teflon Langmuir trough (27.5 cm × 6.25 cm × 0.63 cm) equipped with two identical mobile Teflon barriers (l=6.25 cm). This enables symmetric compression or expansion of monolayers spread at the air-water interface, thereby increasing or reducing the surface pressure, respectively. All isotherms were run with a linear compression speed of 0.1 mm/s. A Wilhelmy balance (Reigler and Kirstein, Berlin, Germany) is used to measure surface pressure. The maximal working surface area of the trough was 145 cm^2 and the water subphase volume used was 95 ml. Subphase temperature was maintained within 0.5 °C of the desired temperature with a homebuilt control station comprised of thermoelectric units (Marlow Industries, Dallas, TX) joined to a heat sink held at 20 °C by a Neslab RTE-100 water circulator (Portsmith, NH). The subphase temperature was monitored by a submerged Teflon-coated thermistor (Omega Engineering Inc., Stanford, CT). A piece of indium tin oxide coated glass (Delta Technologies, Dallas, TX) which can be resistively heated was placed over the trough and held at a temperature to suppress evaporative losses, minimize convective currents, and prevent condensation of water on the microscope objective.

The Langmuir trough is mounted on x, y, and z translation stages (Newport, Irvine, CA) that permit scanning along the air-water interface. The trough assembly is fixed to a custom-built microscope stage to allow simultaneous fluorescence microscopy with a 50× extralong working distance objective (Nikon Y-FL, Fryer Company, Huntly, IL). A high pressure mercury lamp is used for fluorescence excitation, with excitation wavelengths between 530 and 590 nm and emission wavelengths between 610 and 690 nm corresponding to TR-DHPE gathered with a dichroic mirror/filter cube (Nikon HYQ Texas Red, Fryer Company, Huntly, IL). Images from the fluorescence microscope were collected at a rate of 30 frames/s using a charge-coupled device camera (Stanford Photonics Inc., Palo Alto, CA), and recorded on a Sony digital video cassette with a recorder (Sony, Tokyo, Japan). This assembly permits monolayer morphology to be observed over a large lateral area while isotherm data are being obtained. The Langmuir trough and fluorescence microscope apparatus are set on a vibration isolation table (Newport, Irvine, CA) and controlled using a custom software interface designed using LABVIEW 6.1 (National Instruments, Dallas, TX).

TABLE I. Details of poloxamer architecture.

Poloxamer	MW (g/mol)	N_{PEO}[a]	N_{PPO}	N_{PEO}/N_{PPO}
F65	3 400	19	29	1.31
F84	4 200	19	43	0.88
F123	5 750	20	69	0.58
F85	4 620	26	40	1.30
F88	12 000	109	41	5.32
F105	6 500	36	46	1.29

[a]Number of PEO monomers in each of the two hydrophilic chains.

D. Critical micelle concentration experiments

Using a method previously described, the critical micelle concentration (CMC) of each poloxamer was determined by measuring its surface activity at the air-water interface as a function of concentration.[13] Aliquots of 200 mg/ml poloxamer solution were added incrementally to the water subphase, allowed 30 min of equilibration time, and surface pressure was then measured. When there were no further increases in surface pressure, this indicated a poloxamer concentration at which equilibrium was established between the poloxamer population adsorbed to the air-water interface and the population in the subphase; at this point, subsequent addition of poloxamer leads to the formation of micelles and therefore this concentration is defined as the CMC.

E. Lateral compression experiments

All experiments were performed at 30 °C on pure water. In pure lipid compression experiments, the lipid monolayer was spread by dropwise addition of the spreading solution on the water surface, and the organic solvent was allowed to evaporate for 15 min. The barriers were then compressed and isotherm measurements in the form of surface pressure (mN/m) versus area per lipid molecule ($Å^2$/molecule) were taken at 1 s intervals until the system reached its compres-

sion limit. The isotherm provides information about the phase behavior of the monolayer as a function of lipid packing density.

F. Pretreatment experiments

Pretreatment experiments were carried out to test the inserted poloxamer's ability to maintain its position in the lipid monolayer matrix at high lipid packing densities during compression. As in previous experiments, the subphase was heated to 30 °C, DPPC was spread at the interface at a low surface density ($\pi \sim 0$ mN/m), and allowed to equilibrate for 15 min while solvent evaporated. Poloxamer was then injected into the subphase and left to equilibrate for 5 min. The film was subsequently compressed to collapse, and the resulting isotherm of the system was compared to that when no poloxamer was present to determine at which surface pressure the poloxamer was squeezed out of the lipid film. In the context of an electroporated cell membrane, this serves as a model for the healing process when the poloxamer is squeezed out upon regaining the integrity of the membrane.

G. Fluorescence microscopy

During the course of all compression experiments, FM images of the surface morphology were recorded on digital videotape. Due to steric hindrance, the fluorescent molecule, TR-DHPE, partitions into the fluid region, rendering it bright and the condensed phase dark, allowing phase information to be extracted.[19]

H. Model system

To describe the complex mixtures of interest we use the simplest model system that encompasses the main physical behavior of the components forming the poloxamer-lipid mixture. The lipid-lipid interactions are modeled using a two-dimensional truncated-shifted Lennard-Jones potential. This is the simplest interaction form that shows the same three phases of the lipid: gas, liquid expanded, and condensed phases. The explicit form of the potential of interaction is

$$U(r_{ll}) = \begin{cases} U_{LJ}(r_{ll}) - U_{LJ}(r_c) & \text{if } r_{ll} \leqslant r_c \\ 0 & \text{otherwise,} \end{cases}$$

with

$$U_{LJ}(r) = 4\varepsilon\left[\left(\frac{\sigma_{ll}}{r}\right)^{12} - \left(\frac{\sigma_{ll}}{r}\right)^{6}\right], \tag{1}$$

where ε measures the strength of the attraction in the potential and σ_{ll} is a measure of the size of the lipids. Since the interaction potential represents the average of the interactions between the lipids, it should be understood as a potential of mean force.[20] As such, the parameters ε and σ_{ll} should be density and temperature dependent. However, we neglect that effect (see Sec. IV). We consider ε to be the temperature scale. Namely, we consider a scaled temperature in the simulations given by $T^* = k_B T/\varepsilon$.

The interactions of polymer molecules can be divided into two parts, one that arises from the hydrophilic blocks and the other from the hydrophobic blocks. The hydrophilic blocks interact only within themselves since there are no lipids that protrude to the water enough to interact with the long PEO chains. The effective interaction between these blocks is determined from the exact potential of mean force (PMF) between two polymer molecules with one of their ends located at the surface. This PMF is the exact potential between two polymer chains when the distance between the grafting points of the two molecules is d, averaged over all the conformations of both molecules. As it has been demonstrated in earlier work,[21] this potential can be calculated from a large sample of single chain conformations. Namely, the average interaction is determined over the ensemble average of the single chain conformations when the two chains are not interacting with each other.

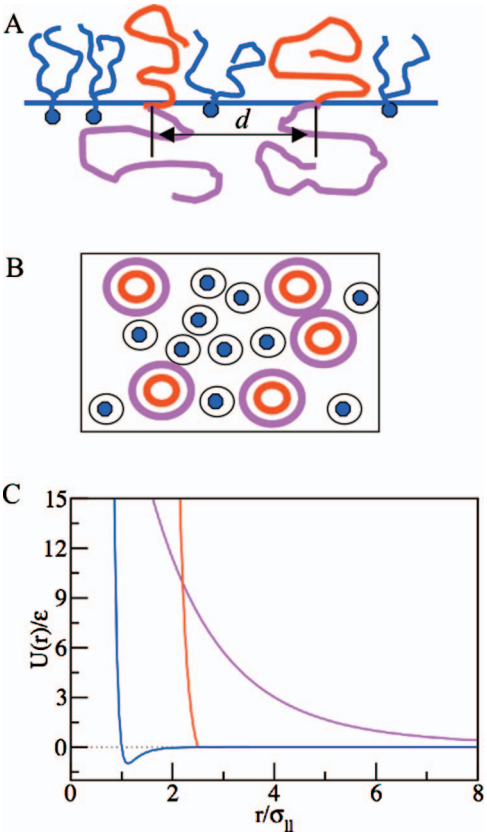

FIG. 2. (Color) (A) Schematic representation of the lipid polymer mixture viewed from the side. (B) Top view of simulated system. The particles are allowed to move only in the two-dimensional plane, with the potential of interactions containing the information on the role of the third dimension. (C) Lipid-lipid (blue curve), lipid-polymer (red curve), and polymer-polymer (magenta curve) potentials used in the calculations presented below. The polymer in this case corresponds to $N_{PEO}=100$.

More explicitly, the effective potential is given by the expression[21]

$$\langle U_{inf}(d)\rangle = -k_B T \ln\left\langle \exp\left[-\beta \sum_1 \sum_2 u_{ij}(r_{ij}(\alpha_1,\alpha_2;d))\right]\right\rangle_{\alpha_1,\alpha_2}, \tag{2}$$

where d is the distance between the junction point of the diblock at the interface, see Fig. 2. The sums run over all the hydrophilic segments of polymers 1 and 2. $u_{ij}(r_{ij})$ is the interaction between segment i of molecule 1 when its confor-

mation is α_1 and segment j of molecule 2 when its conformation is α_2. Namely, $\Sigma\Sigma u_{ij}(r_{ij})$ represents the total intermolecular interaction, and its Boltzmann factor is averaged in the ensemble of all the conformations of the two chains when they do not see each other.

The intersegment interaction is modeled with a truncated and shifted Lennard-Jones (LJ) potential to represent polymers in a good solvent environment. The $\langle\ \rangle$ denote canonical averages over all the independent conformations of molecules 1 and 2. Namely, the average is calculated over an ensemble of conformations of molecules 1 and 2 when they do not interact with each other. This provides a simple way to determine the effective potential.[21]

To calculate the pmf, we have carried out Monte Carlo simulations of a single chain grafted by one end to a planar surface. The surface is located at the plane $z=0$. The chain is modeled as a string of N_p beads, with the position of the first bead fixed at the origin of the coordinates system. The beads are connected by bonds of fixed length σ_{ll} and all the beads (except the first) are restricted to have $z>0$. Excluded volume interaction is accounted for by preventing nonbonded beads to have a separation smaller than σ_{ll}. The configurational space of the grafted chain is sampled using standard Metropolis Monte Carlo. With this model chain, two types of moves are possible. First, the bead at the free end can change the bond angle at random. Second, any internal bead can rotate around the segment connecting its two adjacent beads. The move is accepted if the new position has no overlap with the other beads and if the new z coordinate is positive. A Monte Carlo step is defined as N_p attempts to move a bead chosen at random. For every N_p Monte Carlo steps, a conformation is stored on disk.

Once the set of conformation has been created, the pmf is calculated. Each conformation is taken as a possible conformation for chain 1, and also a possible conformation for chain 2 once the coordinates have been translated a distance d on the xy plane at a random angle. We have calculated the PMF for chains of 50 and 100 beads using 2 000 000 and 5 000 000 randomly chosen different pairs of conformations, respectively. The final potential for each chain length is fitted to an equation of the form

$$U_{\mathrm{mf}}(d) = A_1(N)e^{-d/B_1(N)} + A_2(N)e^{-d/B_2(N)} + 4\varepsilon\left(\frac{\sigma_{ll}}{d}\right)^{12}, \tag{3}$$

where the coefficients are all positive and depend on the chains' molecular weight. The double exponential form contains the soft long-range nature of the potential between the tethered chains in good solvent.

The soft long-range repulsion is the dominant interaction between the polymer chains and therefore they completely dominate the interpolymer interactions, while the main role of the hydrophobic block is to interact with the lipids. The lipid-polymer interaction is assumed to be of the same form as the lipid-lipid interactions. However, due to the different chemical structure of the propylene oxide of the poloxamer as compared to the linear methylenic chain of the lipids, we assume that there is a size mismatch between the polymers and the lipids. As we have shown the size mismatch is one of the necessary conditions for the corralling of the lipids, we will use $\sigma_{lp}=2.5\sigma_{ll}$ throughout the calculations.[17]

The complete set of interactions is shown in Fig. 2 together with a schematic representation of the poloxamer-lipid simulated system. The energy is reported in units of ε, and the length unit is σ_{ll}. The cutoff distance for the lipid-lipid and lipid-polymer interactions is $2.5\sigma_{ll}$. This cutoff for the lipid-polymer potential implies that there is no attractive term, see Fig. 2. We have shown that the presence of an attraction between the lipids and the polymers does not change either the corralling of the lipids or the structure of the aggregates.[17] Namely, the clusters and their structures are very similar whether the cutoff in the LJ interactions between the lipid and the polymers is at $2.5\sigma_{ll}$ or at $5.0\sigma_{ll}$. Therefore, for computational convenience we have chosen to use the cutoff shown in Fig. 2. The fitted parameters for the pmf are as follows: $\sigma=\sigma_{ll}$, $A_1(50)=192.106$, $A_2(50)=3.906$, $B_1(50)=1.048\,53$, $B_2(50)=3.6186$, $A_1(100)=229.309$, $A_2(100)=11.1916$, $B_1(100)=1.3142$, $B_2(100)=4.0184$ [see Eq. (3)].

It should be noted that the model systems presented correspond to diblock copolymers and not the triblock copolymers studied experimentally. We have carried out simulations for model triblocks. These molecules were modeled using all the interactions explained above, but with added constraints that each molecule had two PEO chains by adding an elastic interaction between them. In this way, there is an optimal inter-PEO distance (determined by the length of the PPO block) and deviations from it have an energy penalty modeled as a spring. The results of the simulations with the triblocks have shown no qualitative differences with the results presented here in terms of the cluster formation, the pressure jump upon polymer addition, and the overall structure of the mixture. However, the computational demand of the triblock polymers is much larger and therefore we decided to keep the systematic studies to the diblock systems. As it will be shown in the following sections, the good qualitative agreement between the experimental observations and the Monte Carlo results justifies, *a posteriori*, this choice. A more molecular description of the system is left for future work. However, a more detailed description will require the choice of a limited number of conditions to study, due to the much larger computational effort needed. Thus, the particular model system that we choose to simulate in this work is one that optimizes the computational demand with molecular details. As it will be shown, we believe that the combination of simulations with experimental observations provides better understanding of the molecular features that determine the behavior of lipid-poloxamer mixtures.

I. Monte Carlo simulations

The Monte Carlo simulations are aimed at mimicking the experimental observations on the pressure-area isotherms. Therefore we need to consider a system that can account for the lack of solubility of the lipid in the water subphase and the finite solubility and adsorption energy of the poloxamer. To this end, we perform simulations at a con-

stant number of lipids, constant temperature, constant area, and constant chemical potential of the polymers. The initial condition of the simulations is a system of total area $A=3120\sigma_{ll}^2$ that has $N_l=1000$ lipid molecules at a temperature $T^*=k_BT/\varepsilon=0.8$. The lipid concentration is low as it is the case in the experimental systems. Once the pure lipids reach equilibrium, we allow the adsorption of the polymers at the given chemical potential μ. The types of Monte Carlo (MC) moves that are used include the following: (1) local moves of lipids and polymers. For the local moves we use the Metropolis criteria, i.e., a randomly chosen particle is moved in a random direction and the move is accepted according to

$$\mathrm{acc}(i \to f) = \min(1, \exp[-\beta \Delta U]), \tag{4}$$

where i is the original and f is the final state of the particle, and ΔU is the difference in energy between the two states, which is calculated from the potential of interactions defined above. (2) Attempted insertions (deletions) of polymers. A random number is generated, if it is smaller than 0.5, we attempt to insert a particle. A random position on the surface is chosen and the interaction of a ghost polymer particle with the system is calculated, $\Delta U(N_p \to N_p+1)$. Then the insertion is accepted using the criteria[22]

$$\mathrm{acc}(N_p \to N_p + 1) = \min\left(1, \frac{A}{N+1} \exp[\beta\mu - \beta \Delta U(N_p \to N_p + 1)]\right). \tag{5}$$

If the random number generated is larger than 0.5, then a randomly chosen polymer is a candidate for removal, and it is removed according to the acceptance criteria

$$\mathrm{acc}(N_p \to N_p - 1) = \min\left(1, \frac{N}{A} \exp[-\beta\mu - \beta \Delta U(N_p \to N_p - 1)]\right). \tag{6}$$

We attempt an insertion or deletion of polymer every 50 MC steps. A MC step is defined as an attempt to move each particle in the system once.

After the initial adsorption of the polymers we run the system for a large number (500 000) of MC steps (and insertion/deletion of polymers). This is aimed to ensure that at the given area the system is equilibrated. After a production run of 500 000 MC steps, we compress the layer by changing its area by 1%. The system is equilibrated and a new production run is repeated for the new area at constant N_l, μ, and T. The compression is continued until the smallest desired area is achieved.

It should be noted that the compression simulations are very long since they require the equilibration of systems at many different areas. A typical compression simulation is run for 130 different areas. The two-dimensional pressure at each area per lipid is calculated using the exact virial equation for the pressure, which is given by[23]

$$\Pi = \rho k_B T + \frac{\langle \Sigma_i^N \mathbf{F}_i \cdot \mathbf{R}_i \rangle}{2A}$$

where ρ is the total density of the molecules, $\mathbf{F}_i$ is the instantaneous force on particle i, $\mathbf{R}_i$ is the position of particle i, the dot denotes scalar product $\langle\ \rangle$ denote ensemble average, and A is the total area of the surface.

III. RESULTS

A. Critical micelle concentration results

Experiments to determine the cmc for each poloxamer were performed as previously described;[13] the cmc's for F65, F84, F123, F85, F88, and F105 are approximately $2.17\times10^{-4}M$, $2.01\times10^{-4}M$, $1.46\times10^{-4}M$, $1.94\times10^{-4}M$, $1.02\times10^{-4}M$, and $1.76\times10^{-4}M$, respectively. The concentration of poloxamer used for all of the pretreatment experiments was well below the critical micelle concentration to ensure that poloxamers added would be adsorbed to the air water interface and not dissolved in the subphase in the form of micelles. For each poloxamer pretreatment experiment, 50 μM of polymer was added to the subphase. Therefore, regardless of the molecular weight or $N_{\mathrm{PEO}}:N_{\mathrm{PPO}}$ ratio of the poloxamer, an identical number of poloxamer molecules had the potential to adsorb to the air-water interface and interact with the lipid monolayer.

B. Isotherm comparison

Isotherms and surface morphology measurements were performed to determine the effect of the addition of each poloxamer to the DPPC monolayer. This experimental series aimed at elucidating how the structure of a triblock copolymer, particularly the ratio of the length of the hydrophilic PEO sections to that of the hydrophobic PPO center section, defined as $N_{\mathrm{PEO}}:N_{\mathrm{PPO}}$ (number of PEO subunits:number of PPO subunits), affects the poloxamer's adsorption to the interface and its ability to remain incorporated within the lipid monolayer. The poloxamers used varied in the number of PEO and PPO subunits, $N_{\mathrm{PEO}}:N_{\mathrm{PPO}}$ ratio, and total molecular weight (Table I). All changes in surface morphology and compressibility as shown in the isotherm during the pretreatment experiments compared to those for pure lipid could then be attributed to the addition of poloxamer. A representative lipid isotherm and its parallel poloxamer pretreatment experiment in Fig. 3(A) contain information specific to each polymer in terms of the equilibrium spreading pressure upon adsorption and the subsequent squeeze-out from the monolayer upon compression.

Figure 3(B) shows the pressure-area isotherms as obtained from the MC simulations for the pure model lipids and for the case in which the polymer is added to the lipid layer at a large area per lipid. It is clear from the isotherms that predictions from the simulations are similar to the observed experimental behavior. Upon adsorption of the polymer, there is a jump in the surface pressure; the size of the jump depends on the polymer chemical potential (for experiments, the $N_{\mathrm{PEO}}:N_{\mathrm{PPO}}$ ratio) as will be described below. There is a relatively large range of areas per lipid where the surface pressure of the mixture does not change much upon

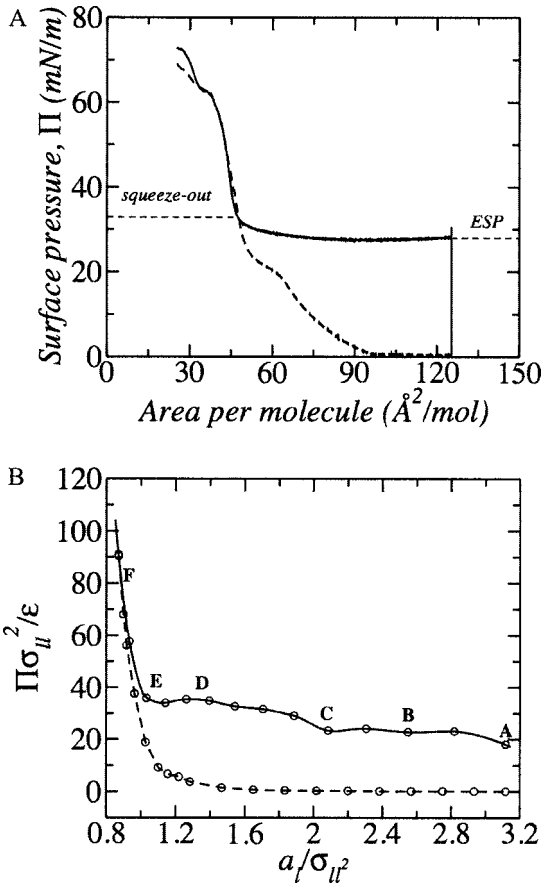

FIG. 3. (A) Lateral compression isotherms of DPPC (dashed line) and DPPC pretreated with F65 (straight line) on water at 30 °C. At $\pi \geqslant 34$ mN/m, the isotherm of the poloxamer pretreated system overlaps with that of pure lipid, indicating squeeze-out of poloxamer from lipid monolayer. (B) Monte Carlo predictions for the pressure-area isotherms for pure model lipid (dashed line) and lipids in the presence of adsorbed polymer (straight line). The polymer corresponds to $N_{PEO}=100$ and chemical potential $\mu=100\varepsilon$. The pressure is measured in units of $\varepsilon/\sigma_{ll}^2$ and the area per lipid in σ_{ll}^2. The letters denote the areas shown in Fig. 6.

compression, and at small areas per lipid the isotherm becomes identical to that of the pure lipid, indicating squeeze-out of the poloxamer molecules.

It should be stressed that the pure lipid as modeled in the MC simulations is not aimed to provide a complete phase diagram of real lipids. It is clear from the simplicity of the model that its main purpose is to provide three possible phases, capturing the main features of the gas, liquid expanded, and condensed phases found in the experimental systems.

C. Equilibrium spreading pressure

The addition of poloxamer to the subphase beneath the DPPC monolayer results in the partitioning of the poloxamer to the air-water interface, giving rise to an instantaneous increase of surface pressure from 0 mN/m to that of the ESP of each poloxamer (Table II). The ESP varies depending on the $N_{PEO}:N_{PPO}$ ratio. A relatively larger hydrophilic PEO block (compared to PPO) translates to a higher hydrophilicity resulting in a lesser amount of poloxamer at the interface and thus a lower ESP. When the $N_{PEO}:N_{PPO}$ ratio is kept constant, in the case of F65, F85, and F105, the ESP scaled

TABLE II. Comparison of equilibrium spreading pressure and squeeze-out pressure based on polymer architecture.

Poloxamer	ESP[a] (mN/m)	Squeeze-out pressure (mN/m)
F65	28	34
F84	33	41
F123	41	45
F85	31	40
F88	23	33
F105	35	42

[a]Equilibrium spreading pressure.

higher with the molecular weight of the poloxamer, demonstrating that smaller poloxamer molecules dissolve more easily into the subphase. Since the overall hydrophilicity of each poloxamer is the same, this indicates that the smaller unimers are better able to shield their hydrophobic PPO block from water.

For the experimental portion, the chain lengths for both blocks have been changed and we present here results pointing to the role of the hydrophobic (PPO) chain length, the hydrophilic (PEO) chain length, and also the overall chain length at a fixed hydrophilic to hydrophobic ratio in determining the lipid/polymer interaction. The simulated model, however, includes explicitly only the PEO chain length through the effective long-range repulsion. The size of the PPO enters through the polymer chemical potential. Namely, the magnitude of μ is a measure of the adsorption energy. As a first approximation we can write the chemical potential of the polymer being linearly dependent on the chain length of each of the blocks, $\mu=a+bN_{PEO}+cN_{PPO}$. Therefore, at constant N_{PEO}, a higher μ, or chemical potential, implicitly implies a longer chain length of the hydrophobic PPO portion of the poloxamer. This enables us to make direct comparisons with experimental observations on the role of the length of each block.

Figure 4 displays the ESP as a function of the polymer chemical potential. As it is done in experimental observations, we define the ESP as the pressure that is calculated in the layer upon adsorption of the polymers at a large area per

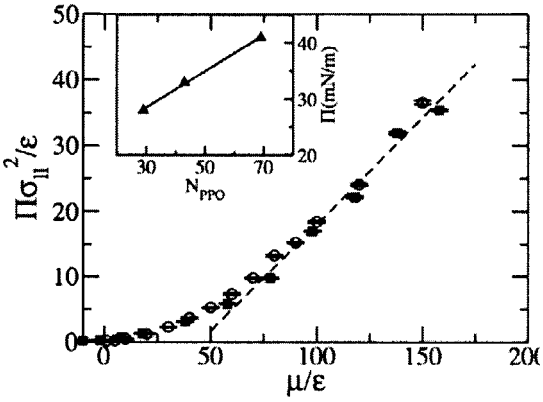

FIG. 4. The equilibrium spreading pressure, determined from MC simulations, as a function of the polymer chemical potential for $N_{PEO}=100$ (circles) and $N_{PEO}=50$ (squares). The chemical potential for $N_{PEO}=50$ is scaled according to the linear approximation described in the text. The inset shows the experimental observations of ESP for the three cases in which $N_{PEO}=29$.

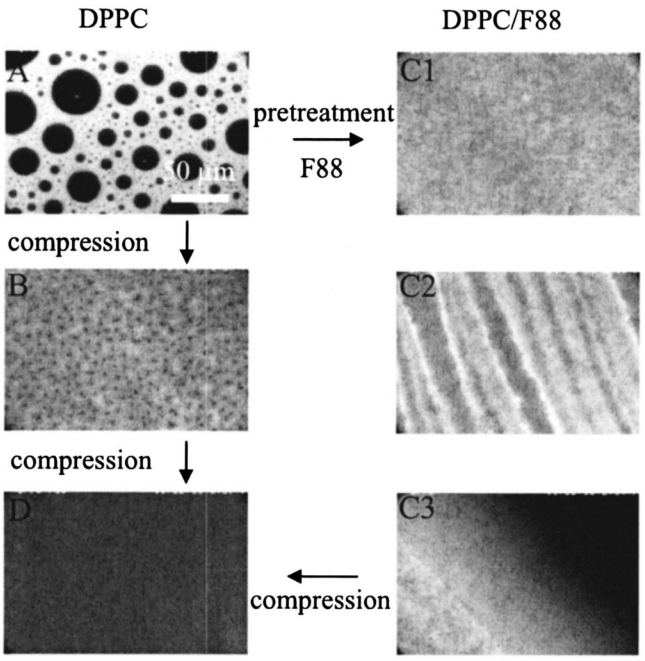

FIG. 5. Fluorescence images comparing DPPC compression (left) and DPPC/F88 pretreatment (right). (A) DPPC in gas/LE coexistence at 125.3 Å^2/mol and ~0 mN/m, and (B) DPPC in LE/C coexistence at 21.5 mN/m and a nominal area of A_{DPPC}=50.8 Å^2. Note that all C micrographs were taken from same monolayer under the same conditions, but from different areas; DPPC after F88 injection at 22.6 mN/m and a nominal area of A_{DPPC}=125.3 Å^2. (C1) DPPC-rich region; (C2) Nonuniform gray phase due to mixing of poloxamer and DPPC; (C3) millimeter-scale dye-excluded regions (top right of figure) are poloxamer rich; (D) DPPC in C phase at 58.39 mN/m and a nominal area of A_{DPPC}=37.82 Å^2. Post-squeeze-out of the F88 poloxamer (33 mN/m), the film is homogeneous and identical to a pure DPPC film. The width of each micrograph is 220 μm.

lipid molecule. The two chain lengths simulated seem to show a universal behavior, as can be seen by the overlap between the two curves when the chemical potential is scaled, assuming a linear dependence of μ in PEO chain length as suggested above. The spreading pressure increases with increasing chemical potential. This is due to the larger number of adsorbed polymers as the chemical potential increases. At low μ, the change in spreading pressure is small; with increasing chemical potential there is a sharp increase in ESP that seems to depend linearly on the polymer chemical potential. This is very similar to the experimentally observed behavior as shown in the inset of Fig. 4 for three different poloxamers of fixed N_{PEO} and varying N_{PPO}.

It should be mentioned that the slope of the experimental and simulation curves should not be compared since they use different units. Furthermore, the simplicity of the model used for the polymer in the simulations makes a quantitative comparison meaningless. However, the fact that the observed behavior is the same indicates that our simple model captures the main physical properties of the lipid-poloxamer mixtures.

D. Morphological changes induced by poloxamers

When the DPPC monolayer is at a large nominal area per molecule (A_{DPPC}=124 Å^2), it is in a gas/liquid-expanded (LE) phase coexistence regime with the gas phase appearing dark and the LE phase bright as seen by FM [Fig. 5(A)]. At 30 °C, DPPC has a phase transition at ~20 mN/m where there is a LE/condensed (C) phase coexistence [Fig. 5(B)] with dark C domains that grow quickly in size. The low contrast between the two phases is due to a roughening at the boundary between liquid-expanded and condensed phases caused by differing elastic properties of the two phases.[24] Upon further compression, the morphology as seen with FM is uniformly gray [Fig. 5(D)].

The addition of the poloxamer to the subphase and its subsequent adsorption to the interface induces a number of morphological changes to the monolayer, namely, compression or coralling of the lipid. Adsorption of the poloxamer at the air/water interface causes the monolayer, initially in the gas/LE phase with dark gaseous domains uniformly distributed in a bright LE monolayer [Fig. 5(A)], to immediately condense into a LE/C coexistence [Fig. 5(C1)] even at a high nominal area per lipid molecule. Furthermore, a separate poloxamer rich phase emerges within the lipid rich areas and there is a degree of heterogeneity, possibly due to the physical incorporation of poloxamer within the lipid matrix [Fig. 5(C2)]. There are also large (up to tens of millimeters) dye-excluded regions composed of adsorbed polymer in coexistence with this lipid LE/C gray phase [Fig. 5(C3)]. The dye-excluded regions have been attributed to poloxamer rich areas while the brighter phases arise from the corralled, lipid rich areas as described by x-ray reflectivity and grazing incidence diffraction experiments.[15,16]

During compression of the pretreated monolayer, the squeeze-out of poloxamer can be visualized via FM; this occurs first with the disappearance of the large scale dye-excluded regions [seen in Fig. 5(C3)] followed by the gray lipid phase becoming more homogenous at the pressure associated with poloxamer squeeze-out [Fig. 5(D)]. Our observations indicate that the millimeter size polymer rich regions are the first to be squeezed out, followed by the poloxamer molecules that are more closely associated with the lipid matrix. Similar morphological changes were seen in all poloxamer systems tested regardless of the N_{PEO}:N_{PPO} ratio or molecular weight, but the amount of large scale dye-excluded polymer phase and the degree of heterogeneity within the condensed phase depended on the ESP of the poloxamer: the lower the ESP, the less dye-excluded polymer rich regions, but the higher the degree of heterogeneity within the lipid region.

E. Corralling

While FM images show the effect of poloxamer interactions with the monolayer on a microscopic scale, MC simulations provide insight to likely molecular arrangements of lipids and polymers. First we analyze the structure of the lipid-polymer mixture at different values of the area per lipid molecule. Figure 6 shows snapshots at the A–F points marked in the isotherm of Fig. 3(B). As the polymers adsorb to the monolayer, there is the formation of lipid domains packed at local high densities surrounded by the polymers. This corralling effect is observed in the simulations instantaneously upon adsorption of the polymers (see simulation movie in the Supplementary Information).[28] The different

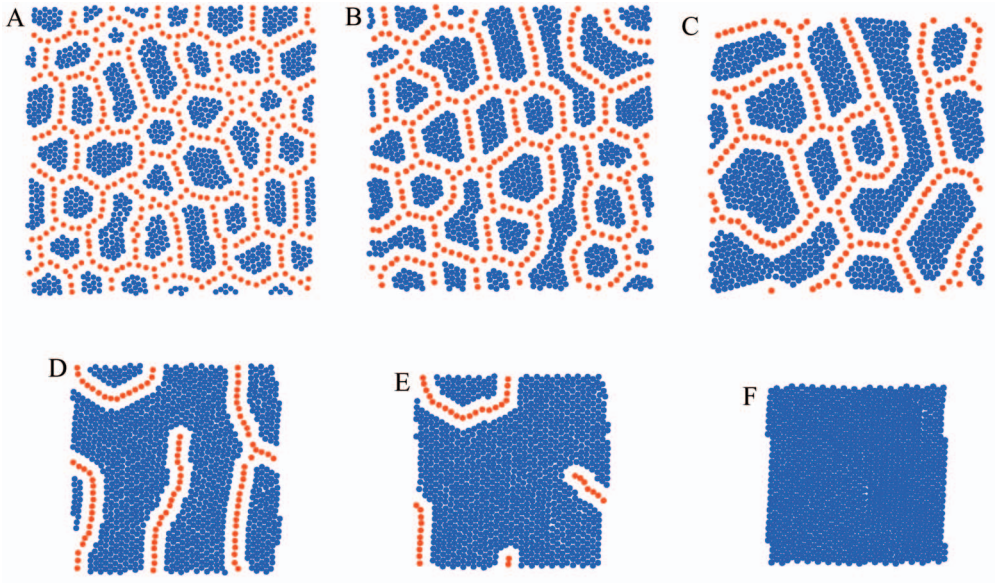

FIG. 6. (Color) Snapshots from the MC simulations at different areas per lipid. The letters correspond to the points denoted in the isotherm, Fig. 3(B). The blue symbols represent the lipids, while the red represent the polymers.

snapshots show that as the layer is compressed, the number of polymer molecules decreases and the size of the clusters increases, until the squeeze-out pressure is reached where the layer is then composed of highly ordered pure lipids.

The specific structures observed in the simulation snapshots show a quasi one-dimensional arrangement of the polymers. Furthermore, the distance between the polymers is smaller than the distance between the lipids and the polymers. To understand these two findings we need to look at the potential of interactions between the different species, Fig. 2. First, the formation of clusters as opposed to macrophase separation or complete miscibility is due to three competing interactions. The polymer-polymer soft repulsion would prefer to have a completely disperse polymer population in the lipid environment, maximizing the distance between polymers and thus minimizing the repulsions. On the other hand, the size mismatch between the lipids and the polymers favors complete phase separation. The structures obtained are the compromise between the two. The exact shapes of the clusters and the surrounding polymers depend on the specific conditions. Second, the one-dimensional structures occur because in all the cases shown the number of polymers is relatively small, and therefore the optimal structure is one in which each polymer has two polymer neighbors at short distances from each other, enabling the maximal number of contacts between the lipids within their clusters. Recall that the mixture's optimal structure is the corralled lipids.[17] The reason that short distances between the polymers are allowed is that the repulsion between the polymers is soft, see Fig. 2. Therefore, a small number of neighbors with relatively large repulsions allow for a large number of lipid-lipid contacts, optimizing all the interactions within the given conditions, see Fig. 2 and Ref. 17.

When the polymers adsorb at a very large area per lipid, the polymers still corral the lipids within regions, but a large number of neighboring polymers are at large distance from each other, as it is shown in the snapshot in Fig. 7. This case corresponds to the adsorption of polymers at an area per lipid that is a factor of 2 larger than that of point A in Figs. 3(B) and 6. The compression of the system in Fig. 7 is the one shown in the isotherm of Fig. 3(B). The large area in Fig. 7 enables the adsorption of a large number of polymers that can corral the lipid into compressed clusters, but without the need of forming lines because the average distance between polymers can be large. Thus, there are only weak repulsions between the polymers. Note that upon compression the polymers will desorb from the surface rather than have a large repulsion with other polymers, thus driving the formation of the lines. It should also be mentioned that we have checked the corralling effect by the polymers if the hard-core repulsion between the polymers is shifted to larger distances and we have found no qualitative difference with the results presented here.

All of the different conditions that we have studied with

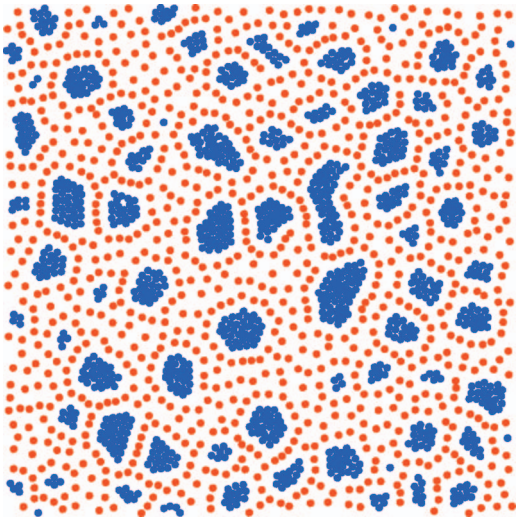

FIG. 7. (Color) Same as Fig. 6, but for an area per lipid $a_l=6.67\sigma_{ll}^2$.

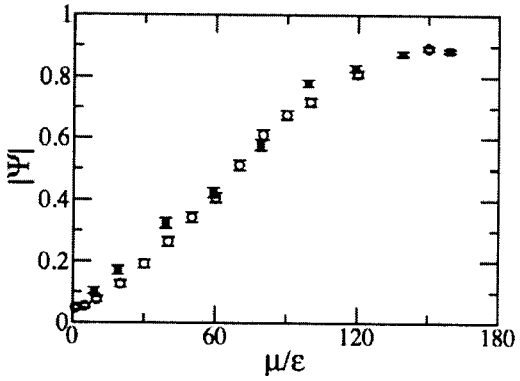

FIG. 8. The local order parameter as a function of the polymer chemical potential. All the conditions and symbols are the same as Fig. 4.

simulations show the same qualitative picture as presented in Figs. 3(B) and 6; namely, a jump to the ESP upon adsorption in which the polymers corral the lipids, and a region of almost constant pressure where the polymers desorb, accompanied by an increase in the size of the lipid clusters. As we have discussed in previous work,[17] the clusters are obtained as long as there is a mismatch in the size of the hydrophobic block of the polymer and that of the lipid, and there is the presence of long-range soft repulsions between the hydrophilic blocks. The qualitative features observed in the simulation are in line with the experimental observations and they provide a molecular-level understanding of the possible structures formed upon polymer adsorption.

F. Lipid local order

To gain some insight into the role of the polymer chemical potential on the structure of the corralled lipid clusters upon polymer adsorption, we define the local order parameter

$$|\Psi| = \frac{1}{M}\sum_{l=1}^{M} |g_6(l)|, \quad g_6(l) = \frac{1}{n(l)}\sum_{j} \exp[6i\theta_{lj}],$$

where θ_{lj} is the angle between the interparticle (lj) vector and a reference axis. $n(l)$ is the number of neighbors within a cluster and M is the total number of lipids considered. We consider lipids that are not at the boundary of the cluster and therefore only lipids with $n(l)>3$ are considered. We have used this convention because otherwise the boundary lipids have too much weight on the final result, even though they are not representative of the order *within* the cluster. The quantity $|\Psi|$ takes the value 0 for a random distribution of angles and 1 for a perfect hexagonal lattice. Thus, the closer the value to unity, the more ordered the cluster. Figure 8 shows the order parameter as a function of the polymer chemical potential for the same N_{PEO} cases shown in Fig. 4. A proper comparison between the experimental observations and the simulations should be done on the region where the equilibrium spreading pressure is linear in the PPO chain length. Thus, we need to consider the range in which $\mu/\varepsilon > 100$. In this range the order parameter is very high and the clusters are highly ordered, with crystal-like local order. This is very much in line with the previous x-ray scattering experiments that showed that the corralled lipids exhibit the same order as in the liquid condensed phase.[15,16]

Figure 9 shows snapshots of the corralled lipids upon adsorption of the polymer for three different values of the chemical potential. The snapshots present a more graphical view of the results presented in Fig. 8. In all cases these polymers corral the lipids, forming clusters whose crystal-like order increases with increasing chemical potential of the polymer. As μ increases, the amount of adsorbed polymer is larger, and thus the local density within the lipid clusters increases. This provides a detailed picture of the effect of the $N_{PEO}:N_{PPO}$ ratio on the corralling of lipids. The larger local density within the aggregates induces the larger degree of order observed.[25]

G. Pretreatment and squeeze-out

To compare experimentally how different poloxamer structures, specifically the $N_{PEO}:N_{PPO}$ ratio, affect its interactions of poloxamer with a lipid monolayer, the number of monomers of the PEO block was held constant at $N_{PEO}=19$ for both blocks while the size of the PPO center block was varied: $N_{PPO}=29$ for F65, $N_{PPO}=43$ for F84, and $N_{PPO}=69$ for F123. A representative pretreatment experiment of DPPC and F65 is shown in Fig. 3(A) from which the ESP and the squeeze-out pressure can be determined. F65 was squeezed out at 34 mN/m, F84 at 41 mN/m, and F123 at 45 mN/m (Table II). Thus, a larger PPO block in poloxamers with the same $N_{PEO}:N_{PPO}$ ratio helps maintain the poloxamer within the lipid monolayer up to a higher surface pressure. This is likely because the larger hydrophobic center block interacts more strongly with the tail region of the lipid, and hence faces a higher energy barrier for squeeze-out. As a result, a higher pressure was required for squeeze-out. By changing the size of the hydrophobic PPO block, this series of experiments has also varied the overall hydrophobic character $(N_{PEO}:N_{PPO})$ of the poloxamer. Therefore, the effects arising

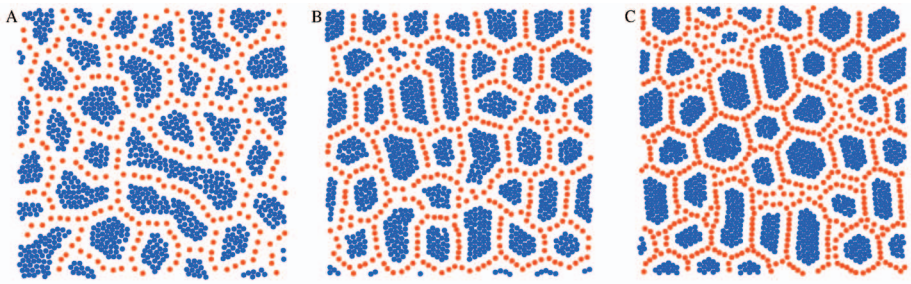

FIG. 9. (Color) Snapshots from the MC simulations for three different values of the chemical potential of the polymer. (A) $\mu/\varepsilon=70$, (B) $\mu/\varepsilon=100$, and (C) $\mu/\varepsilon=150$. The calculations are for $N_{PEO}=100$. The symbols are as in Fig. 6.

from varying the N_{PPO} length and changing the overall hydrophilicity (N_{PEO}:N_{PPO}) of the poloxamer molecules need to be identified and separated.

Alternatively, if the length of the PPO block is held constant, increasing the length of the PEO (hydrophilic) block increases the propensity for the polymer to be squeezed out as shown by a lower squeeze-out pressure. The poloxamer F85 (N_{PEO}=26, N_{PPO}=40) is squeezed out of the DPPC monolayer at 40 mN/m while the larger F88 molecule (N_{PEO}=109, N_{PPO}=41) is only maintained within the monolayer up to a surface pressure of 33 mN/m. Increasing the overall hydrophilic character of the poloxamer by lengthening the PEO block lowers the squeeze-out pressure, indicating that the N_{PEO}:N_{PPO} ratio is the primary indicator for poloxamer maintenance within the monolayer.

When the N_{PEO}:N_{PPO} ratio is held constant but the molecular weight is varied, a larger polymer has a higher squeeze-out pressure from the monolayer. Previous work by Maskarinec and Lee using a series of poloxamers with N_{PEO}:N_{PPO}=5.25 has shown that larger polymers, with consequently larger central hydrophobic subunits, maintain their position within the monolayer up to higher surface pressures and lipid packing density.[14] Because this effect could be attributed to the sheer large size of the polymer compared to that of the phospholipids (F108, MW of 11 400; F118, MW of 14 600), a constant N_{PEO}:N_{PPO} series using F65 (MW =3400), F85 (MW=4620), and F105 (MW=6500) was performed. A similar increase in squeeze-out pressure scaling with molecular size was seen (Table II).

Results from the pretreatment experiments indicate that the ability of a poloxamer molecule to stay within a lipid monolayer at high pressure is an interplay between the ratio of the subunit block lengths and the size of the molecule. On the one hand, a poloxamer with a relatively larger PEO block has a lower squeeze-out pressure, while one with a relatively larger PPO block has a higher squeeze-out pressure. On the other, increasing the size of both PEO and PPO blocks (while keeping the N_{PEO}:N_{PPO} ratio constant) raises a poloxamer's squeeze-out pressure.

The last comparison between computer simulations and experimental observations could be done for the squeeze-out pressure. This is a much harder quantity to determine from the simulations for two reasons. First, the full isotherms take a very large amount of computer time. We have complete isotherms for only a selective number of cases. Second, as can be seen from the isotherm presented in Fig. 3(B) the exact determination of the squeeze-out pressure is problematic and the number of polymers close to the squeeze-out pressure becomes very small (see Fig. 6). With these limitations in mind, we have calculated the squeeze-out pressures for polymers with N_{PEO}=100 and found that it increases with increasing chemical potential, $\Pi\sigma_{ll}^2/\varepsilon$=28.93 and 41.89 for μ/ε=80 and 100, respectively, in line with the experimental observations for the cases with constant length of PEO and increasing the chemical potential, and thus the effective size, of PPO, see Table II.

IV. DISCUSSION AND CONCLUSIONS

The driving force behind this work is to further understand how the structure of poloxamers affects their interactions with a lipid monolayer, specifically by examining the insertion of the polymer at low lipid density followed by its expulsion upon compression to a high lipid density. We have examined the effect of poloxamer structure by changing the length of each PEO or PPO chain relative to the other, as well as changing the total size of the polymer with a constant N_{PEO}:N_{PPO} ratio.

This was achieved experimentally with pretreatment experiments to determine equilibrium spreading pressure and squeeze-out pressure of poloxamers of varying structure, and computationally with Monte Carlo simulations of a coarse-grained lipid/polymer system where N_{PEO} and the chemical potential could be altered. To fully understand all the energetic contributions from each molecule in the system, detailed atomistic molecular dynamics calculations could be run, but this computationally intensive technique would not capture the dynamic behavior of the poloxamer/phospholipid mixture on a relevant time scale. To access the spectrum comparable to experiment, coarse-grained models were used as representations of the molecules and their interactions. The main aim of coupling experiments with simulations was to decipher the basic physical behavior responsible for the experimental observations. Experimentally, the ESP of poloxamers was shown to vary depending on the N_{PEO}:N_{PPO} ratio, with more hydrophilic molecules having a lower ESP due to greater solubility and less material at the interface. The effect of overall size of the poloxamer was measured (the N_{PEO}:N_{PPO} ratio was kept constant in this case) with smaller molecules resulting in a lower ESP. Using Monte Carlo simulations, we have presented parallel results where the ESP also scales with chemical potential, and thus the effective block size, in a similar fashion.

Results from the simulations shed light on the possible picture of rearrangement and expulsion of poloxamer molecules upon compression of the monolayer as the condensed domains of lipid molecules become larger. This is echoed in FM images of the poloxamer-lipid mixed film. Addition of poloxamer to the subphase of a DPPC monolayer at high nominal area per lipid molecule causes a pressure jump to above the onset of the LE/C phase transition, causing a corralling of lipids to pack tightly. At the same time, the adsorbed poloxamers are found to be phase separated from the lipids, giving rise to large dye-excluded regions in the film. Upon compression, the poloxamer-rich regions are squeezed out and the gray phase becomes uniform again, providing visual evidence (also supported by isotherms) that the poloxamer has been excluded from the film.

Local order or degree of crystallinity of the corralled lipid domains has been quantified for polymers of different chemical potential. An increase in chemical potential results in an increase in the order parameter of the lipid molecules. This can been seen as a corollary to increasing the length of the central PPO block, therefore raising the ESP which in turn increases the degree to which the lipids are corralled or condensed in the lipid-rich regions.

Pretreatment experiments have been performed to determine the effect of poloxamer structure and length on the interaction of the polymers with the lipid monolayer. The $N_{PEO}:N_{PPO}$ ratio or the degree of overall hydrophilicity of the molecule proves important, with relatively longer PEO chains (more hydrophilic) resulting in a lower squeeze-out pressure and a relatively longer PPO block (more hydrophobic) having a higher squeeze-out pressure. For a polymer inserted in the lipid matrix, its solubility in the subphase is determined by interplay between being maintained at the interface with its hydrophobic block interacting with the acyl chains of neighboring lipid molecules, and being dissolved into the subphase so as to minimize the PEO-PEO repulsive interaction as the nominal area per molecule gets smaller. More hydrophobic poloxamers with longer PPO chains are less soluble in the subphase and have a greater physical interaction with the lipid tail region at the interface and therefore can be maintained within the monolayer to a much higher pressure. Conversely, if the N_{PPO} is held constant, the change in solubility due to lengthening the water soluble PEO chains dramatically lowers the squeeze-out pressure. If the hydrophilicity of the poloxamer is kept constant, the squeeze-out pressure scales with the size of the molecule. While one may be tempted to infer that this is primarily due to a larger PPO central block and therefore more interaction with neighboring molecules or more steric hindrance upon squeeze out, it should be noted that the ESP, hence solubility, also scales similarly with poloxamer size. The simulation results parallel those found for experiments with squeeze-out pressure scaling with chemical potential, suggesting that the course-grained model captures the nuances of the mixed polymer-lipid monolayer system.

We have shown how the ratio of hydrophilic:hydrophobic portions of a triblock copolymer affects its interactions with a lipid monolayer upon adsorption and subsequent squeeze-out. Qualitative agreement between experiment and simulation has been shown for various systems and measurements suggesting that the simulations provide insight into the driving forces of lipid/polymer interactions. These results can be used as predictive tools for designing poloxamers of certain $N_{PEO}:N_{PPO}$ ratios and lengths for specific cellular targets within biological systems.

One of the cell's natural mechanisms of healing membrane disruption is exocytosis, a process in which an intracellular lipid vesicle moves to the plasma membrane and subsequent fusion ensues.[26] In the case of injury, production of these vesicles could be hampered or simply could not be maintained at a rate necessary to seal the permeabilized layer. The poloxamer thus provides a stop-gap measure under such circumstances. Our pretreatment experiments indicate that polymer association with the damaged layer and subsequent lipid corralling is immediate upon the introduction of the polymer in the vicinity of the compromised film. Squeeze-out of the poloxamer, on the other hand, occurs upon membrane "healing" when a certain critical density of phospholipid has been achieved and provides a graceful way for the polymer to exit the membrane when it is no longer needed. Moreover, amphiphilic F68 molecules have been shown to help a protein refold into its native conformation after thermal denaturation[27] suggesting that not only could the poloxamer assist with membrane sealing, but it might also play a role in the recovery of other biologically relevant molecules within the membrane that were damaged in the process.

ACKNOWLEDGMENTS

One of the authors (S.L.F.) is grateful for the support of a National Science Foundation graduate research fellowship. One of the authors (K.Y.C.L.) acknowledges supports from the David and Lucile Packard Foundation (99-1465), the University of Chicago MRSEC Program of the National Science Foundation under award DMR0213745, and a NSF/SCRIF junior faculty grant (CHE/9816513). One of the authors (I.S.) acknowledges support from the National Science Foundation under award CTS-0338377. Two of the authors (S.L.F. and D.Z.) contributed equally to this work.

[1] I. R. Schmolka, J. Am. Oil Chem. Soc. **54**, 100 (1977).
[2] G. S. Kwon, Crit. Rev. Ther. Drug Carrier Syst. **20**, 357 (2003).
[3] E. Bilensoy, M. A. Rouf, I. Vural, M. Sen, and A. A. Hincal, AAPS PharmSciTech **7**, 38 (2006).
[4] D. W. Murhammer and C. F. Goochee, Biotechnol. Prog. **6**, 142 (1990).
[5] R. C. Lee, L. P. River, F. S. Pan, L. Ji, and R. L. Wollmann, Proc. Natl. Acad. Sci. U.S.A. **89**, 4524 (1992).
[6] F. A. Merchant, W. H. Holmes, M. Capelli-Schellpfeffer, R. C. Lee, and M. Toner, J. Surg. Res. **74**, 131 (1998).
[7] B. Greenbaum, K. Blossfield, J. Hannig, C. S. Carrillo, M. A. Beckett, R. R. Weichselbaum, and R. C. Lee, Burns **30**, 539 (2004).
[8] G. Serbest, J. Horwitz, and K. Barbee, J. Neurotrauma **22**, 119 (2005).
[9] S. Yasuda, D. Townsend, D. E. Michele, E. G. Favre, S. M. Day, and S. M. Metzger, Nature (London) **436**, 1025 (2005).
[10] Y. Wang, S. Liu, C. Y. Li, and F. Yuan, Cancer Res. **65**, 7541 (2005).
[11] H. Möhwald, Annu. Rev. Phys. Chem. **41**, 441 (1990).
[12] C. Ege and K. Y. C. Lee, Biophys. J. **87**, 1732 (2004).
[13] S. A. Maskarinec, J. Hannig, R. C. Lee, and K. Y. C. Lee, Biophys. J. **82**, 1453 (2002).
[14] S. A. Maskarinec and K. Y. C. Lee, Langmuir **19**, 1809 (2003).
[15] G. H. Wu, J. Majewski, C. Ege, K. Kjaer, M. J. Weygand, and K. Y. C. Lee, Phys. Rev. Lett. **93**, 028101 (2004).
[16] G. H. Wu, J. Majewski, C. Ege, K. Kjaer, M. J. Weygand, and K. Y. C. Lee, Biophys. J. **89**, 3159 (2005).
[17] D. S. Zhang, M. A. Carignano, and I. Szleifer, Phys. Rev. Lett. **96**, 028701 (2006).
[18] L. C. Chang, C. Y. Lin, M. W. Kuo, and C. S. Gau, J. Colloid Interface Sci. **285**, 640 (2005).
[19] C. M. Knobler, Science **249**, 870 (1990).
[20] D. Chandler, *Introduction to Modern Statistical Mechanics* (Oxford University Press, New York, 1987).
[21] V. Harismiadis and I. Szleifer, Mol. Phys. **81**, 851 (1994).
[22] D. Frenkel and B. Smit, *Understanding Molecular Simulation: From Algorithms to Applications*, 2nd ed. (Elsevier, New York, 2002).
[23] D. A. McQuarrie, *Statistical Mechanics* (Harper and Row, New York, 1976).
[24] H. Diamant, T. A. Witten, C. Ege, A. Gopal, and K. Y. C. Lee, Phys. Rev. E **63**, 061602 (2001).
[25] The results presented in Figs. 8 and 9 are similar to the ones previously published in Ref. 17. We include them here to present a complete picture of the structures that would correspond to the different regions studied in the experimental systems, and how the simulation results relate to those experiments.
[26] R. A. Steinhardt, G. Bi, and J. M. Alderton, Science **263**, 390 (1994).
[27] A. M. Walsh, D. Mustafi, M. W. Makinen, and R. C. Lee, Ann. N.Y. Acad. Sci. **1066**, 321 (2005).
[28] See EPAPS Document No. E-JCPSA6-127-022732 for a Monte Carlo simulation of the poloxamer adsorption into the lipid layer followed by the compression of the layer and expulsion of the polymers. This document can be reached through a direct link in the online article's HTML reference section or via the EPAPS homepage (http://www.aip.org/pubservs/epaps.html).